Ecotoxicology
DOI 10.1007/s10646-011-0659-4

Assessing abalone growth inhibition risk to cadmium and silver by linking toxicokinetics/toxicodynamics and subcellular partitioning

Wei-Yu Chen · Yun-Ru Ju · Bo-Ching Chen · Jeng-Wei Tsai · Chia-Jung Lin · Chung-Min Liao

Accepted: 17 March 2011

Abstract The purpose of this study was to link toxicokinetics/toxicodynamics and subcellular partitioning for assessing the susceptibility and the growth inhibition risks of abalone *Haliotis diversicolor supertexta* exposed to waterborne and foodborne cadmium (Cd) and silver (Ag). We reanalyzed published data on growth inhibition and subcellular partitioning associated with the present mechanistic model to explore the correlations among elimination (k_e), detoxification (k_d), and recovery (k_r) rate constants and to assess the growth inhibition risk. We found a positive correlation among k_e, k_d, and k_r in abalone exposed to Ag. We also employed a life-stage based probabilistic assessment model to estimate the growth inhibition risk of abalone to environmentally relevant Cd (5–995 μg l^{-1}) and Ag (0.05–9.95 μg l^{-1}) concentrations in Taiwan. The results showed that abalone had a minimum 20% probability of the growth inhibition risk exposed to Cd, whereas Ag exposure was not likely to pose the risk. The maximum biomasses were estimated to be 0.0039 and 0.0038, 61.61 and 43.87, and 98.88 and 62.97 g for larvae, juveniles, and adults of abalone exposed to the same levels of Cd and Ag, respectively. Our study provides a useful tool to detect potential growth biomass of abalone populations subjected to Cd and Ag stresses and mechanistic implications for a long-term ecotoxicological risk assessment in realistic situations.

Keywords Abalone · Cadmium · Silver · Bioaccumulation · Subcellular partitioning · Growth inhibition risk

W.-Y. Chen · Y.-R. Ju · C.-J. Lin · C.-M. Liao (✉)
Department of Bioenvironmental Systems Engineering, National Taiwan University, Taipei, Taiwan 10617, Republic of China
e-mail: cmliao@ntu.edu.tw

B.-C. Chen
Department of Post-Modern Agriculture, MingDao University, Changhua, Taiwan 52345, Republic of China

J.-W. Tsai
Graduate Institute of Ecology and Evolutionary Biology, China Medical University, Taichung, Taiwan 40402, Republic of China

Introduction

With its delicacy and high market values, abalone is an important aquaculture product worldwide. The farming regions of abalone are widely distributed thought Australia, New Zealand, Chile, China, Taiwan, and the United States (Oakes and Ponte 1996; Jarayabhand and Pahavasit 1996; Gordon and Cool 2001). *Haliotis diversicolor supertexta* is the most abundant abalone species in Taiwan with feeding of red algal *Gracilaria* spp. to attain the best growth conditions (Chen 1989). Positive evidence showed that contaminants affected ecophysiology of marine organisms, such as growth, reproduction, and survival capacities (Ng and Wood 2008). Hence, the water quality is a most important determinant for regulating the health of abalone (Slaveykova and Wilkinson 2005; Wang and Rainbow 2006).

Cadmium (Cd) and silver (Ag) are non-essential metals to aquatic organisms. Both of them inhibit Ca^{2+} and Na^+/K^+-ATPase activity by decreasing the active uptake capacities of Ca^{2+} and Na^+ in tissues of aquatic organisms (Morgan et al. 1997; Bury and Wood 1999; Castilho et al. 2001). Cd and Ag toxicities in seawater are far less known than in freshwater. Their toxicities were also associated with the bioavailable concentrations rather than with the total metal concentrations. The toxic metals could enter

Published online: 25 March 2011

aquatic organisms via water and food and accumulate in subcellular compartments of tissues, controlling by geochemical and physiological factors, such as ions, salinity, food appetites, and ingestion behaviors (Rainbow 2002; Nichols et al. 2006; Pan and Wang 2008).

Waterborne metals rely on passive diffusion from ambient water via the gill into the tissue. Foodborne metal is a significant exposure route affecting the accumulation in marine animals and further in food chains via trophic transfer (Rainbow et al. 2007). The interactions among waterborne and foodborne metals and target tissues of aquatic organisms play an important role in the risk assessment of aquatic ecosystems, yet numerous studies only investigated the accumulative capacities in one of these pathways, which is not enough to fully describe the exposure situations for aquatic organisms.

Lee et al. (2002) proposed the damage assessment model (DAM), which is capable of describing the time course of median effect concentration data for chemicals acting through the reversible interaction between chemicals and receptors (Lee et al. 2002; Ashauer et al. 2007). That mechanism well describes the physiological reactions of damage and recovery when organisms are under chemical stress. The DAM describes the occurred hazard based on the cumulative tissue damage reaching a critical level, representing the health state of an organism. However, the DAM did not incorporate the chemical bioavailability to assess the physiological response of organisms.

The concentration of metal ions complex or the amount of metals binding to aquatic organisms are not enough to predict the toxic effect of aquatic organisms. Recent studies indicated that a subcellular partitioning model (SPM) can be used to describe the complex binding of chemical ion in different subcellular compartments with different chemical ion-binding ligands (Wang and Rainbow 2006; Buchwalter et al. 2008; Huang et al. 2008, 2010; Voets et al. 2009; Ng et al. 2009; Seebaugh and Wallace 2009). They pointed out that the metal ions binding to target subcellular compartments could reflect the chemical toxicity. The critical sites of toxic action in subcellular fraction include the metabolically active pool (MAP) comprising organelles (insoluble) and heat sensitive (labile) protein (soluble) and the metabolically detoxified pool (MDP) comprising metal rich granules (insoluble) and metallothionein-like proteins (soluble).

Organisms could fuel ontogenetic growth by allocating absorbed energy to synthesize new biomass and to maintain existing biomass. The West growth model (West et al. 2001) can be used to describe the organism's ontogenetic growth (biomass) trajectory from birth to maturity based on energy allocation without toxicity. On the other hand, the toxicity dynamic energy budget model (DEB_{tox}) can be used to describe the mode of action (MOA) of metal toxicity that alters the energy allocation, including metabolism, growth, and reproduction (Kooijman and Bedaux 1996; Alunno-Bruscia et al. 2009). Hence, the integration of the West growth model and DEB_{tox} theory can effectively predict allometric relationships between the growth rate and the life history events under metal stresses.

It is important to understand the Cd and Ag toxic effects, accumulations, and detoxifications with critical subcellular fractions in aquatic organisms to elucidate the physiological function inhibition in the field risk assessment applications. The purpose of this study was to link toxicokinetics/toxicodynamics and subcellular partitioning to assess the susceptibility and the growth inhibition risks of abalone to environmentally relevant waterborne and foodborne Cd and Ag stresses appraised by recently published experimental data. Moreover, the integration of toxicokinetics/toxicodynamics, detoxification, and bioregulation knowledge can provide a more reliable prediction for a long-term exposure risk assessment in field situations.

Materials and methods

Study data

The valuable database provided by Huang et al. (2010) offered an opportunity to examine the waterborne and foodborne Cd and Ag toxicities for abalone from a subcellular partitioning perspective. Briefly, Huang et al. (2010) carried out a series of experiments that included accumulation, subcellular partitioning, and body weight growth inhibition. The experiments provided a potential burden-based toxicity assessment to understand the difference between waterborne and foodborne metal toxicities. Therefore, the published data adopted from Huang et al. (2010) were reanalyzed to estimate the key physiological determinants, such as uptake, elimination, and detoxification rate constants.

To determine Cd and Ag accumulation, Huang et al. (2010) conducted four exposure bioassays by using juvenile abalone *H. diversicolor* (mean shell width of 30.9 ± 1.2 mm) exposed to waterborne concentrations of 50 μg l^{-1} Cd (as $CdCl_2$) and 5 μg l^{-1} Ag (as $AgNO_3$), respectively. In the foodborne exposure, the algae *Gracilaria tenuistipitata* var. *liui* were exposed to Cd of 50 and 500 μg l^{-1} and Ag of 5 and 50 μg l^{-1}, respectively. The algae concentrations were 9.56 and 120 μg g^{-1} dry wt Cd and 5.52 and 45.1 μg g^{-1} dry wt Ag as the low and high foodborne exposure treatments, respectively. Exposure bioassays were fed 15 g algae for 7 weeks. The water quality conditions were maintained at temperature 20°C and salinity 31 psu. On the other hand, Cd accumulation

bioassay for algae *Gracilaria coronopifolia* was adopted from Hsieh (2005) with algae exposed to 9.76 mg l^{-1} Cd for 7 days.

Huang et al. (2010) separated five differential subcellular fractions including cellular debris, metal-rich granules (MRG), organelles, heat-denatured protein (HDP), and metallothionein-like protein (MTLP) from soft tissue of three abalones in each exposure experiment. Abalone were dissected to remove their shells. The Cd and Ag subcellular partitioning can be pooled into MAP and MDP. The MDP comprises MRG and MTLP, whereas MAP comprises the Cd and Ag HDP and organelles.

Huang et al. (2010) measured the fresh weight of abalone at 0, 2, 4, and 7 weeks in the above-mentioned exposure experiments to investigate the physiological responses. Then the daily growth inhibition rate was calculated at 0–2, 2–4, 4–7, and 0–7 weeks. Thus, we can obtain an exposure time-specific dose–response curve that can be used to estimate the exposure time-specific median effect dose [ED50(t)].

Toxicokinetic/toxicodynamic model

In light of a biologically DAM, chemicals are acting through a reversible interaction between chemicals and receptors. Chemicals accumulate in aquatic organisms by uptake and elimination mechanisms. Consequently, the tissues were damaged by the internalized chemical concentrations. On the other hand, aquatic organisms can also recover the damaged tissues. The relationships between chemical tissue residue and residue-induced damage can be described by a first-order damage accumulation model and a first-order bioaccumulation model (Lee et al. 2002). Based on the DAM, the damage-based EC50 can be derived as (Lee et al. 2002),

$$\mathrm{EC50}(t) = \frac{D_{\mathrm{E,50}}/k_a}{\left(\frac{e^{-k_r t}-e^{-k_e t}}{k_r-k_e}+\frac{1-e^{-k_r t}}{k_r}\right)} BCF^{-1}, \quad (1)$$

where k_a is the damage accumulation rate (g μg^{-1} d^{-1}), $D_{\mathrm{E,50}}/k_\mathrm{a}$ is a coefficient that reflects the compound equivalent toxic damage level required for median effect (μg d g^{-1}), k_e is the elimination rate constant (d^{-1}), k_r is the damage recovery rate constant (d^{-1}), and BCF is the bioconcentration factor (ml g^{-1}). In the foodborne ED50 prediction, EC50 and BCF are replaced by ED50 and a biomagnification factor (BMF) (g g^{-1}) in Eq. (1).

In the DAM scheme, the accumulation-induced organism damage is proportional to body chemical concentration, whereas the damage recovery is proportional to the cumulative damage from waterborne or foodborne chemicals. The cumulative damage (D_i) can be expressed as (Lee et al. 2002),

$$D_i(t) = k_a \cdot \frac{k_u}{k_e} \cdot C_i \left(\frac{e^{-k_r t}-e^{-k_e t}}{k_r-k_e}+\frac{1-e^{-k_r t}}{k_r}\right), \quad (2)$$

where k_u is the uptake rate constant (ml g^{-1} d^{-1} or g g^{-1} d^{-1}) and C_i is the chemical concentration from waterborne (i = w) or foodborne (i = f) sources. The DAM proposes that the hazard occurs based on the irreversible cumulative damage reaching a critical level.

Base on the DAM, the cumulative hazard [$H(t)$] is proportional to the cumulative damage level as $H(t) = k_3 D(t)$ where $k_3 = k_k/k_a$ is the proportional coefficient between damage (D) and hazard (H) and k_k is the killing rate describing the relationship between cumulative damage and hazard level. k_k can also be calculated as ln2/($D_{\mathrm{E,50}}/k_\mathrm{a}$) (Lee et al. 2002).

Finally, the time-dependent susceptibility probability can be expressed as the exponential of cumulative hazard as (Lee et al. 2002),

$$S_{p,i}(t) = 1 - \exp\left(-k_3 \cdot k_a \cdot \frac{k_u}{k_e} \cdot C_i \left(\frac{e^{-k_r t}-e^{-k_e t}}{k_r-k_e}+\frac{1-e^{-k_r t}}{k_r}\right)\right), \quad (3)$$

where $S_{\mathrm{p},i}(t)$ is the susceptibility probability from waterborne or foodborne Cd and Ag.

Detoxification model

Detoxification rate (k_d, d^{-1}) can be estimated followed the metal influx threshold (MIT) concept introduced by Croteau and Luoma (2009). Croteau and Luoma (2009) proposed that MIT occurs when metal influx ≥ the combined rates of metal loss and detoxification. Thus, the external metal uptake in MAP of aquatic organisms exceeds the MAP influx threshold, the metal will be lost and detoxification will be triggered. Based on the MIT perspective, k_d can be calculated as

$$k_d = \frac{k_{u,\,MAP} \cdot C_i}{C_{MAP,0}} - k_e, \quad (4)$$

where k_d is the detoxification rate constant (d^{-1}), $k_{\mathrm{u,\,MAP}}$ is the metal uptake rate from water or food into MAP (ml g^{-1} d^{-1} or g g^{-1} d^{-1}), $C_{\mathrm{MAP,0}}$ is the metal concentration in MAP without metal exposure (control group), and k_e is the elimination rate constant from the internal body into the water (d^{-1}).

Growth toxicity model

Here we integrated the $\mathrm{DEB_{tox}}$ theory and the West growth model to simulate the metal toxicity caused growth (biomass) inhibition curve for abalone populations. MOA of

metal toxicity alters the energy allocation among metabolism, growth, and reproduction. Since more energy transfer to detoxification could induce less energy allocation to growth. Tsai and Liao (2006) also revealed that MOA of reducing food assimilation efficiency could be well-predicted by the West growth model. Here we incorporated a susceptibility probability function into the West growth model to describe the growth inhibition,

$$W(t) = \left[W_{\max,0}\left(1 - S_{p,i}(t)\right)\right] \cdot \left\{1 - \left[1 - \left(\frac{W_0}{W_{\max,0}\left(1 - S_{p,i}(t)\right)}\right)^{1/4}\right] \times \exp\left(-\frac{A_0 t}{4\left(W_{\max,0}\left(1 - S_{p,i}(t)\right)\right)^{1/4}}\right)\right\}^4, \quad (5)$$

where $W(t)$ is the time-dependent body weight (g), W_0 is the body weight at birth of abalone (approximately 3.95×10^{-7} g), $W_{\max,0}\left(1 - S_{p,i}(t)\right)$ is the ultimate body weight of abalone under the contaminated environment where $W_{\max,0}$ is the maximum body weight in an uncontaminated environment (102 g) (Huang 1998), and A_0 is a species-specific growth coefficient ($g^{1/4}$ d^{-1}).

Predictive growth inhibition risk model

To investigate the relationships among biomass growth inhibition of abalone, susceptibility probability, and waterborne and foodborne Cd and Ag exposures, the present study used a biologically based susceptibility probability model together with both exposure pathways ($S_{p,wf}$) to reconstruct the dose–response profile. The relationship between environmental metal concentration and abalone susceptibility has the form of,

$$S_{p,wf}(t) = 1 - \exp\left[-\left(H_w(t) + H_f(t)\right)\right], \quad (6)$$

where $H_w(t)$ and $H_f(t)$ are the cumulative hazard levels from waterborne and/or foodborne Cd and Ag exposures, respectively. Here we adopted Cd and Ag concentration data of abalone cultural ponds in Taiwan regions (Cheng 2004) to implement the proposed model.

The growth inhibition risk can be calculated as the probability density function (pdf) of Taiwan region-specific Cd and Ag concentrations by the conditional probability of Cd and Ag susceptibility ($S_{p,wf}$). Hence, a joint probability function can be used to calculate the risk probability of growth inhibition for body weight,

$$P(R_{BW}) = P(S_{p,wf}) \times P\left(BW \,|S_{p,wf}\right), \quad (7)$$

where $P(R_{BW})$ represents the probability risks for body weight inhibition and $P(S_{p,wf})$ is the pdf of metal susceptibility.

Data analysis and simulation scheme

Salinity is the determinant factor for bioavailable Ag activity concentration. All waterborne Ag activity concentrations were adjusted by a Ag activity coefficient of 0.589 at temperature 25°C and salinity 35 psu (Ward and Kramer 2002).

Toxicokinetic parameters of uptake and elimination rate constants (k_u and k_e) can be estimated by fitting the integrated form of the toxicokinetic (TK) rate equation to exposure data for constant waterborne and foodborne Cd and Ag,

$$C_b(t) = C_{b0}e^{-k_{ei}t} + \frac{k_{ui}}{k_{ei}}C_i\left(1 - e^{-k_{ei}t}\right), \quad (8)$$

where C_{b0} is initial concentration of Cd or Ag in the internal body or MAP of abalone or algae (μg g^{-1} wet wt) and C_b is the metal concentration in internal body or MAP. Here, we adopted the fresh abalone weight growth rate at weeks 0, 2, 4 and 7 that were exposed to waterborne or foodborne Cd and Ag.

We used an empirical equation to describe the general allometric relations among shell width, shell length, and fresh weight (Huang 1998),

$$B = 0.0176 + 0.6848L, \quad (9)$$

$$W = 3.86 \times 10^{-5}L^{3.211}, \quad (10)$$

where B is the shell width (mm), L is the shell length (mm), and W is the fresh weight (g). Then we estimated the fresh weight of abalone at weeks 0, 2, 4, and 7 exposed to waterborne or foodborne Cd and Ag, respectively. We reanalyzed the data of growth inhibition at weeks 0, 2, 4, and 7. Accordingly, a dose–response curve at a specific exposure time can be obtained to estimate the ED50(t).

We used a Hill model to fit the constructed dose-growth inhibition response curve to estimated ED50 values as,

$$R(C_f) = \frac{R_{\max}}{1 + \left(\frac{ED50}{C_f}\right)^n}, \quad (11)$$

where $R(C_f)$ is the foodborne metal dose–dependent growth inhibition response (%), C_f is the foodborne metal dose (μg g^{-1}), $R_{\max}$ is the maximum response (%), and n is the Hill coefficient.

We employed the TableCurve 2D (Version 5, AISN Software, Mapleton, Oregon, USA) and 3D (Version 4, AISN Software, Mapleton, Oregon, USA) to optimal fit the published data to obtain optimal statistical models. The Crystal Ball® software (Version 2000.2, Decisionerring, Inc., Denver, Colorado, USA) was employed to implement a Monte Carlo simulation to obtain 2.5 and 97.5 percentiles as the 95% confidence interval for all fitted models. The growth inhibition risk curves were generated from the

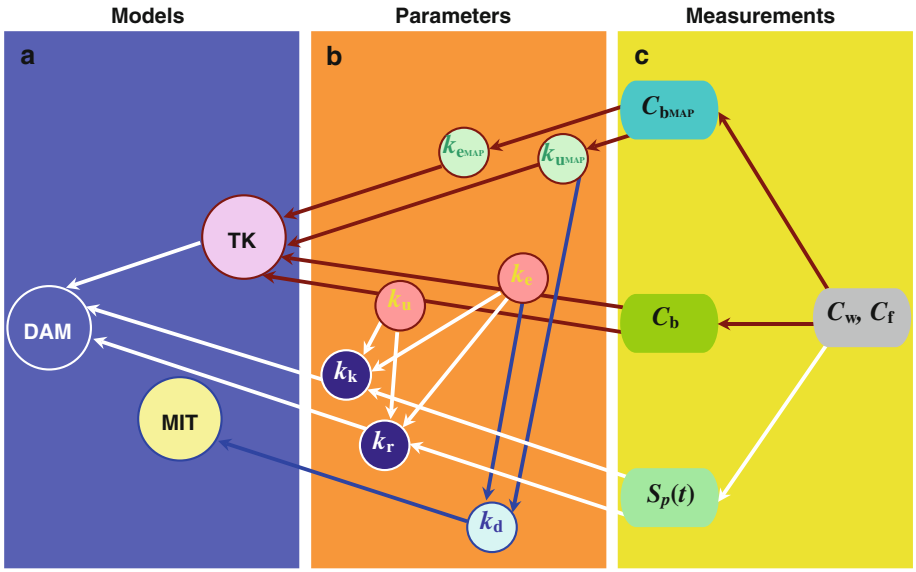

Fig. 1 Schematic showing the relationships among measurements adopted published data, parameter estimations, and corresponding present mechanistic models

cumulative distribution of simulation outcomes. It showed that 10,000 iterations were sufficient to ensure the results. The interactions of measurements used in this study for estimating the key parameters and the present mechanistic models are depicted in Fig. 1.

Results

Biological response of abalone

The rapid accumulation fashion was found in *G. coronopifolia* exposed to 9.76 mg l^{-1} Cd over the course of 7 days (Hsieh, 2005). The toxicokinetic rate equation in Eq. (8) was fitted to Cd accumulation data to obtain the estimated uptake rate constant k_u of 9.40 ± 1.70 ml g^{-1} d^{-1} (mean ± se) and elimination rate constant k_e of 0.64 ± 0.14 d^{-1} ($r^2 = 0.94$) (Fig. 2a). Due to the limitation of time-dependent bioaccumulation data, a parsimonious power law was used to describe the relationships between waterborne Ag concentration and algae tissue concentration as $C_b = 1.27C_w^{0.91}$ ($r^2 = 0.99$) (Fig. 2b).

The toxicokinetic rate equation in Eq. (8) was best fitted ($r^2 = 0.98$) to 49-days exposures data in abalone tissue, resulting in k_u estimates of 490 ml g^{-1} d^{-1}, 0.64, and 0.60 g g^{-1} d^{-1} and k_e estimates of 0.91, 1.06, and 2.09 d^{-1} for waterborne, low foodborne, and high foodborne Cd exposures, respectively (Table 1, Fig. 3a, c, e). In Ag exposures, k_u estimates of 58 ml g^{-1} d^{-1}, 0.004 g g^{-1} d^{-1}, and 0.19 g g^{-1} d^{-1} and k_e estimates of 0.035, 0.054, and 3.01 d^{-1} were obtained with $r^2 = 0.79$, 0.26, and 0.51 for waterborne, low foodborne, and high foodborne Ag exposures, respectively (Table 1, Fig. 3b, d, f).

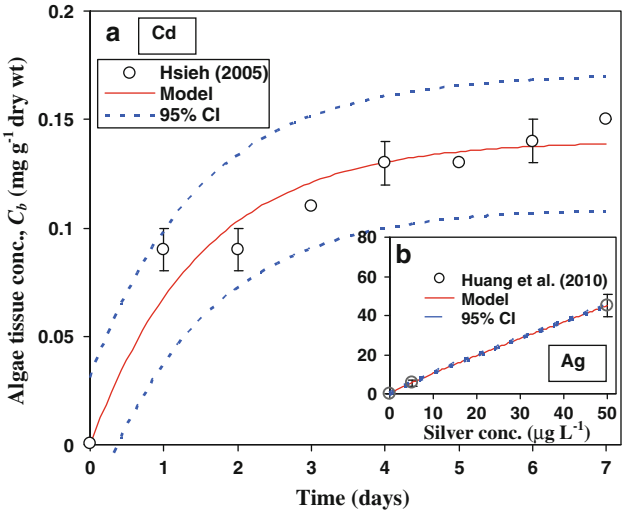

Fig. 2 **a** Fitting toxicokinetic equation [Eq. (8)] to published experimental exposure data in algae exposed to 9.76 mg l^{-1} Cd. **b** A relationship between waterborne Ag concentration and internal concentration of algae

The toxicokinetic parameters of Cd in MAP were estimated to be 310 ml g^{-1} d^{-1}, 0.97, and 1.28 d^{-1} for $k_{u,MAP}$ and 1.15, 2.28, and 2.05 d^{-1} for $k_{e,MAP}$ with $r^2 = 0.22$, 0.43, and 0.32 for waterborne, low foodborne, and high foodborne exposures, respectively (Table 1). For toxicokinetic parameters of Ag in MAP, the $k_{u,MAP}$ estimates were 7890 ml g^{-1} d^{-1}, 7.096, and 6.153 d^{-1} and $k_{e,\ MAP}$ estimates were 5.24 × 10^{-8}, 0.043, and 0.065 d^{-1} with $r^2 = 0.88$, 0.74, and 0.42 for waterborne, low foodborne, and high foodborne exposures, respectively (Table 1).

Our results showed that detoxification did not trigger when abalone were exposed to low foodborne exposure at 9.56 µg g^{-1} Cd, whereas detoxification rate constant k_d

Table 1 Estimated bioaccumulation, damage assessment model (DAM), and metal influx threshold (MIT) parameters of abalone exposed to waterborne and foodborne Cd/Ag

Parameters	Cadmium	Silver
Waterborne		
C_w (μg l^{-1})	50	5
k_{uw} (ml g^{-1} d^{-1})[a]	490 (0.98)[d]	58 (0.79)
k_{ew} (d^{-1})[a]	0.91	0.035
$k_{u,\ MAP}$ (ml g^{-1} d^{-1})[a]	310 (0.22)	7890 (0.88)
$k_{e,\ MAP}$ (d^{-1})[a]	1.15	5.24×10^{-8}
k_k (g μg^{-1} d^{-1})[b]	0.0007 (0.99)	0.016 (0.99)
k_r (d^{-1})[b]	0.196	0.358
k_{dw} (d^{-1})[c]	314.37	314.59
Low foodborne		
C_w (μg l^{-1})	50	5
C_f (μg g^{-1})	9.56 ± 0.51[e]	5.52 ± 1.73
k_{uf} (g g^{-1} d^{-1})[a]	0.64 (0.98)	0.004 (0.26)
k_{ef} (d^{-1})[a]	1.06	0.054
$k_{u,\ MAP}$ (d^{-1})[a]	0.97 (0.43)	7.096 (0.74)
$k_{e,\ MAP}$ (d^{-1})[a]	2.28	0.043
k_k (g μg^{-1} d^{-1})[b]	0.077 (0.67)	0.116 (0.98)
k_r (d^{-1})[b]	3.390	0.420
k_{df} (d^{-1})[c]	–[f]	0.468
High foodborne		
C_w (μg l^{-1})	500	50
C_f (μg g^{-1})	120 ± 1.50	45.1 ± 5.58
k_{uf} (g g^{-1} d^{-1})[a]	0.60 (0.98)	0.19 (0.51)
k_{ef} (d^{-1})[a]	2.09	3.01
$k_{u,\ MAP}$ (d^{-1})[a]	1.28 (0.32)	6.153 (0.42)
$k_{e,\ MAP}$ (d^{-1})[a]	2.05	0.065
k_k (g μg^{-1} d^{-1})[b]	0.037 (0.62)	0.154 (0.66)
k_r (d^{-1})[b]	7.614	3.366
k_{df} (d^{-1})[c]	1.034[f]	0.691

[a] Estimated from Eq. (8)

[b] Estimated form DAM by fitting the safety growth probability

[c] Estimated from MIT mechanism in Eq. (4)

[d] Values are r^2 in the parentheses

[e] Mean ± S.D

[f] Not detected from MIT

was estimated to be 314.37 and 1.034 d^{-1} for waterborne and high foodborne Cd exposures. On the other hand, k_d were estimated to be 314.59, 0.468, and 0.691 d^{-1} for waterborne, low foodborne, and high foodborne Ag exposures, respectively (Table 1). The k_d estimates were found to be increased with increasing of foodborne Ag concentrations.

A Hill model [Eq. (10)] was used to fit the constructed Cd and Ag dose–growth inhibition response to estimate ED50 values. Time-dependent ED50(t) could be estimated by fitting a DAM scheme-based ED50 model [Eq. (1)] to Hill-based ED50(t) data ($r^2 = 0.48$ and 0.53) (Fig. 4a and c). The results indicated that estimated recovery rate constant (k_r) of 6.29 d^{-1} for foodborne Cd exposure was much greater than that of 3.79 d^{-1} for foodborne Ag exposure. The killing rate constants (k_k) were calculated to be 2.24 and 10.79 g μg^{-1} d^{-1} for abalone exposed to foodborne Cd and Ag, respectively.

We used the susceptibility probability model [Eq. (3)] to fit the specific dose or concentration with time-dependent growth inhibition response to obtain model-specific parameters (Table 1). The k_k estimates ranged from 0.0007–0.077 g μg^{-1} d^{-1} of Cd exposures. Those were much lower than that of 0.016–0.154 g μg^{-1} d^{-1} for Ag exposures. The recovery rate constant k_r estimates ranged from 0.196–7.614 and 0.358–3.366 d^{-1} for Cd and Ag exposures, respectively. The predicted EC50 values of waterborne Cd and Ag can also be estimated by incorporating the estimated model parameters (k_k and k_r) into the susceptibility probability model (Fig. 4b and d).

Subcellular Cd/Ag compartmentalization and % detoxified

The relationships between % detoxified in MDP and foodborne metal concentration were shown in Fig. 5. The results showed that % detoxified in MDP increased with increasing of foodborne concentration for both foodborne Cd and Ag exposures. The best equations to describe their relations were $y = 76/(1 + (12.83/x)^{0.25}$ ($r^2 = 0.91$) for foodborne Cd exposure, whereas $y = 17.26 + 0.008x^2$ ($r^2 = 0.99$) for foodborne Ag exposure.

Linkages among ecophysiological determinants

We further explored the correlation between k_e and k_d of Ag exposure. The result showed a positive linear trend with $k_e = -6.16 + 13.27k_d$ ($r^2 = 0.99$) (Fig. 6a). On the other hand, a positive correlation was found for damage recovery capacity (k_r) and elimination capacity (k_e) of Ag exposure with $k_e = -0.343 + 0.996k_r$ ($r^2 = 0.99$) (Fig. 6b). Figure 6c illustrates a response surface that depicts the correlations among k_r, k_e, and k_d with $k_r = 0.157 + 0.974\ k_e + 0.4k_d$ ($r^2 = 0.99$).

Risk assessment practices

A best-fit for the reducing food assimilation efficiency model could demonstrate biomass growth effect of abalone under various metal exposure scenarios with estimated model-specific parameters (growth cost coefficient) ($r^2 = 0.92$–0.96) (Fig. 7a–f). The estimated growth cost coefficients (A_0) ranged from 0.03–0.04 $g^{1/4}$ d^{-1} for Cd exposures and 0.035–0.04 $g^{1/4}$ d^{-1} for Ag exposures,

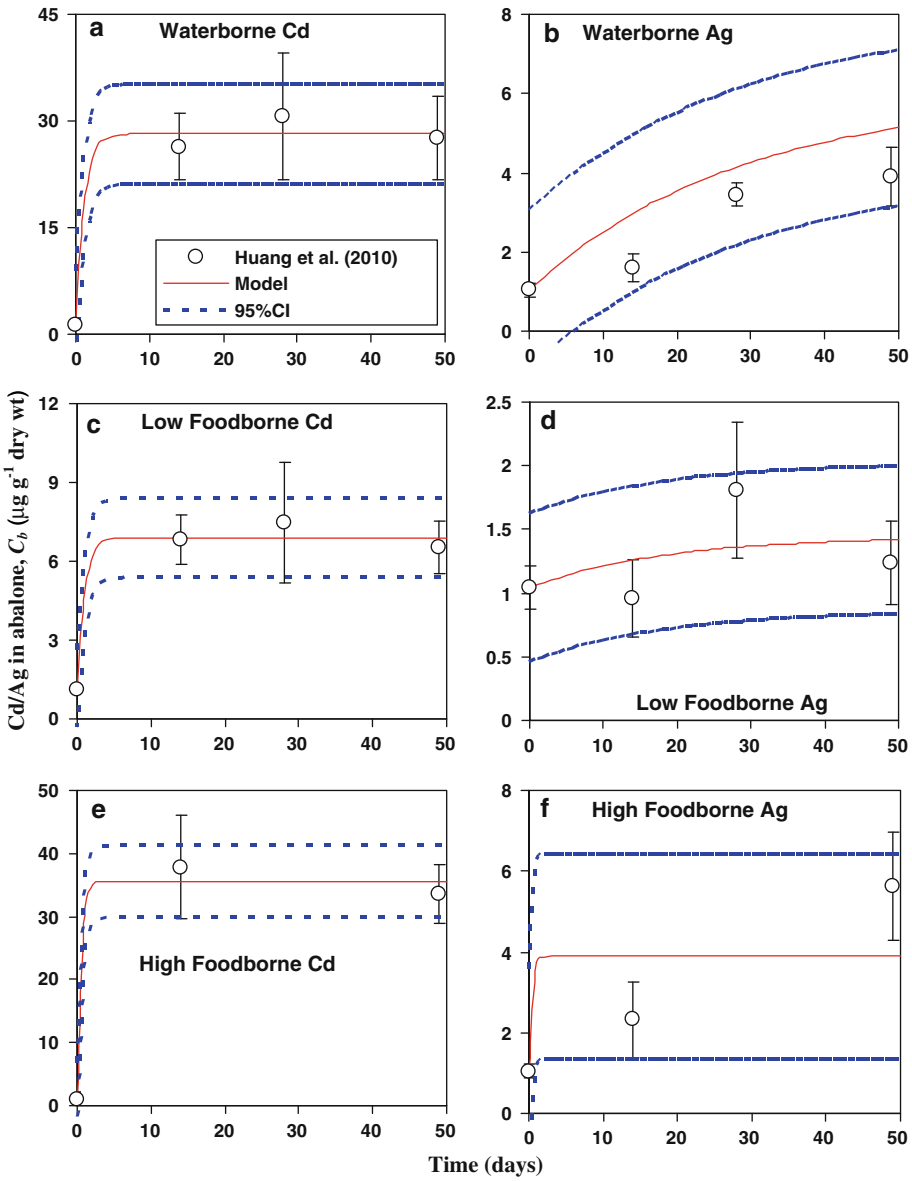

Fig. 3 Fitting toxicokinetic model to published experimental exposure data (mean with SD) in abalone exposed to **a** waterborne 50 μg L^{-1} Cd and **b** 5 μg L^{-1} Ag, **c** low foodborne 9.56 μg g^{-1} Cd and **d** 5.52 μg g^{-1} Ag, and **e** high foodborne 120 μg g^{-1} Cd and **f** 45.1 μg g^{-1} Ag

whereas the value for non-exposure was 0.047 ± 0.003 $g^{1/4}$ d^{-1} (mean ± se) (Fig. 7g). The results indicated that the growth cost coefficient depends on the exposure metal concentrations, revealing that high concentration inhibits much more growth cost. Moreover, waterborne Ag inhibits much more growth than that of waterborne Cd, whereas foodborne Ag inhibits less growth than that of foodborne Cd.

We applied the probabilistic risk assessment model [Eq. (7)] to estimate the potential growth inhibition risk under environmental Cd and Ag concentrations in Taiwan. The fitted lognormal distributions with a geometric mean of 35.26 μg l^{-1} and a geometric standard deviation of 4.6 [denoting as LN(35.26 μg l^{-1}, 4.6)] and LN(3.31 μg l^{-1}, 1.67) were used to describe Cd and Ag exposure concentrations, respectively. On the other hand, the probability distributions of susceptibility for abalone subjected to Cd and Ag exposures at day 200 (juvenile stage) can be calculated as LN(0.072, 4.6) and LN(0.15, 1.67), respectively.

We simulated the relations between body weight and susceptibility of abalone by using the growth toxicity model Eq. (5) with range values of 5–995 μg l^{-1} Cd and 0.05–9.95 μg l^{-1} Ag in Taiwan, respectively (Fig. 8a and b). Abalone growth inhibition risk probability in the Cd and Ag exposure scenarios can be estimated by Eq. (7). The results showed that growth inhibition risk gradually increases as body weight decrease (Fig. 8c and d). Our results indicated that the abalone had a minimum 20% probability of growth inhibition risk exposed to Cd, whereas Ag exposures were not likely to pose a growth inhibition risk. The dynamics of body weight changes in three life-stage of larvae (day 0–25), juveniles (day

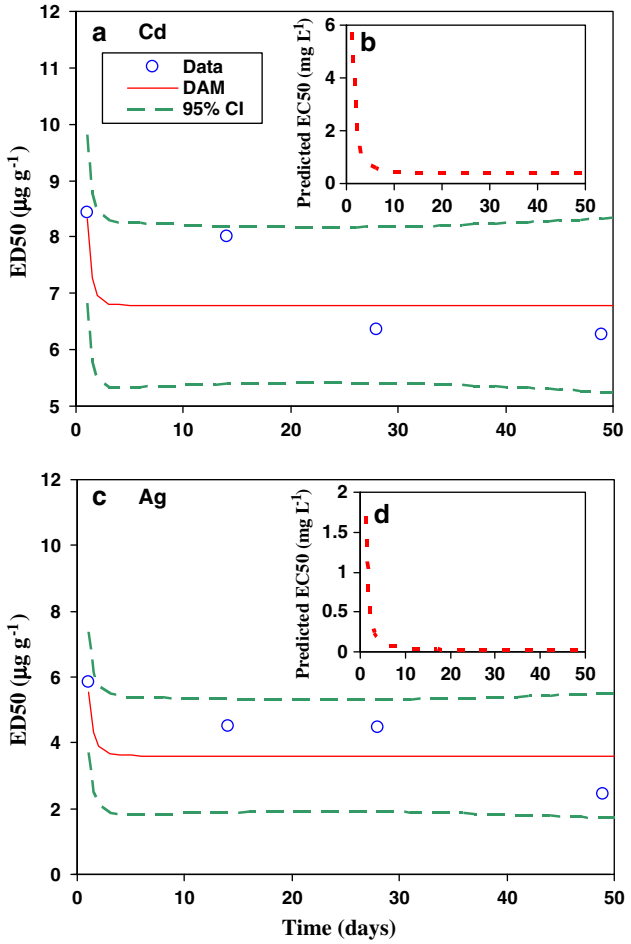

Fig. 4 **a** Fitting the damage-based ED50 model [Eq. (1)] to Hill-based ED50(t) data in foodborne Cd-abalone system. **b** Predicted EC50 based on estimated DAM parameters in waterborne Cd-abalone system. **c** Fitting the damage-based ED50 model [Eq. (1)] to Hill-based ED50(t) data in foodborne Ag-abalone system. **d** Predicted EC50 based on estimated DAM parameters in waterborne Ag-abalone system

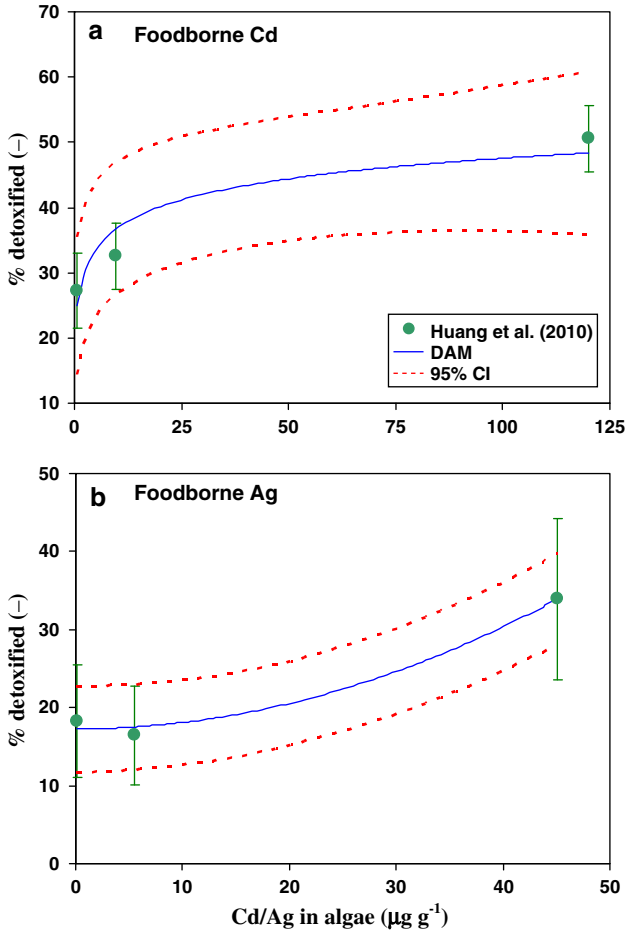

Fig. 5 **a** A relationship between % detoxified of abalone based on subcellular partitioning and foodborne Cd. **b** A relationship between % detoxified of abalone based on subcellular partitioning and foodborne Ag. Error bars represent standard deviation from mean

25–730), and adults (day 730–2,000) subjected to 0–1,000 μg l^{-1} Cd and 0–25 μg l^{-1} Ag can also be simulated (Fig. 8e–j).

Discussion

Effect of seawater and freshwater on metals bioavailability

Trace metal bioavailability in aquatic molluscs was controlled by the multitudinous geochemical components. The seawater ecosystem is completely different from the freshwater ecosystem because of the contents of sodium and chlorine ions, salinity, dissolved organic carbon, and the iono-regulate effect (Wood et al. 2004; Grosell et al. 2007; Nadella et al. 2009). Mclusky et al. (1986), Grosell et al. (2007), and Nadella et al. (2009) further pointed out that the metal toxicity might increase with decreasing of salinity.

In this study, we adopted the major ions concentrations and Ag activity coefficient from Stumm and Morgan (1996) and Ward and Kramer (2002) to take into account metal bioavailability. The predicted metal bioavailable capacities were thus valid at the same salinity circumstance with experimental setting of 35 psu salinity seawater (Huang et al. 2010). In the past decade, cadmium, copper, silver, and zinc- associated biotic ligand models (BLMs) have been well-developed with geochemical modeling and affinity (stability) determinants in freshwater ecosystems (Playle et al. 1993; Janes and Playle 1995; Di Toro et al. 2001; Borgmann et al. 2004), yet the development of a marine BLM for understanding the affinity constants, available competing or complexing ions to target metal, high ionic strength, and metals species in the elaborate marine ecosystem is still limited. The knowledge of

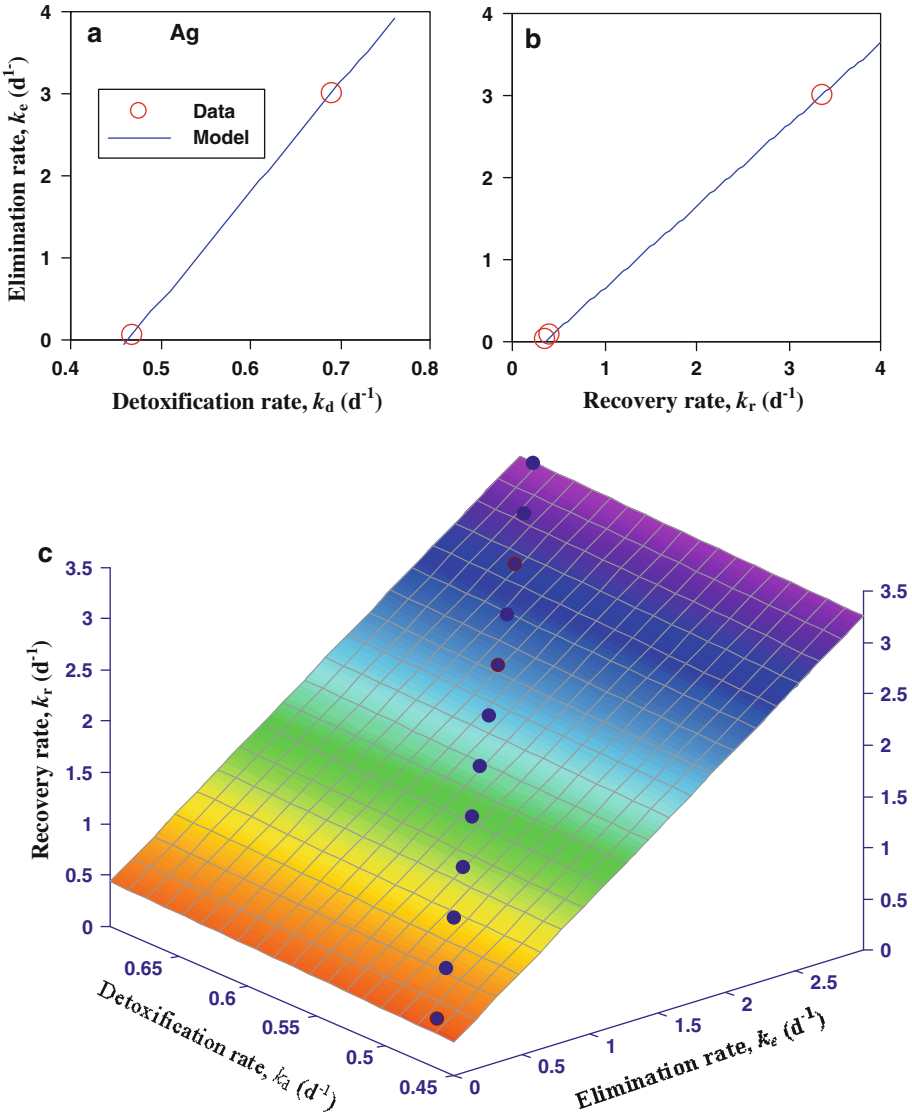

Fig. 6 **a** The best fitted model of the correlation of $k_e - k_d$ and **b** $k_e - k_r$. **c** A response surface representing the correlation among k_r, k_e, and k_d

salinity influence for establishing a critical determinants database of marine BLM that considers salinity influence should be explored. Moreover, the physiological function of marine organisms was different from that of freshwater organisms, since the freshwater organisms were necessitated to actively transport sodium and chlorine ions from water.

Comparison of waterborne and foodborne Cd/Ag toxicity to abalone

In this study, three ecophysiological determinants (k_e, k_d, and k_r) of bioaccumulation and coping mechanisms were integrated to assess Cd and Ag growth susceptibility risk for abalone. However, in the Cd exposure, k_d estimation based on the MIT perspective was not triggered at waterborne Cd of 50 μg l^{-1} and foodborne 5.52–45.1 μg g^{-1}. We also found a positive correlation among k_r, k_e, and k_d in Ag exposure. Therefore, these three ecophysiological determinants do not exist in a compensation relationship when exposed to Cd and Ag.

The rank of waterborne/foodborne Cd accumulation in subcellular fraction in the abalone was cellular debris > MTLP > MRG > HDP ≥ organelles, whereas for waterborne/foodborne Ag it was cellular debris > MRG > organelles > MTLP > HDP (Huang et al. 2010). Generally, metal toxicity was induced by metal sensitive fractions such as organelles and HDP, whereas the fitness was controlled by biological detoxified fractions like MRG and MTLP (Wallace and Luoma 2003; Wang and Rainbow 2006). The biological detoxified fraction to the total cellular accumulation was in the majority for Cd. Additionally, the abilities to repair waterborne/foodborne Cd-induced damage were better than that to recover from waterborne/foodborne Ag-induced damage in abalone. Our results indicated that average k_r of waterborne Cd had

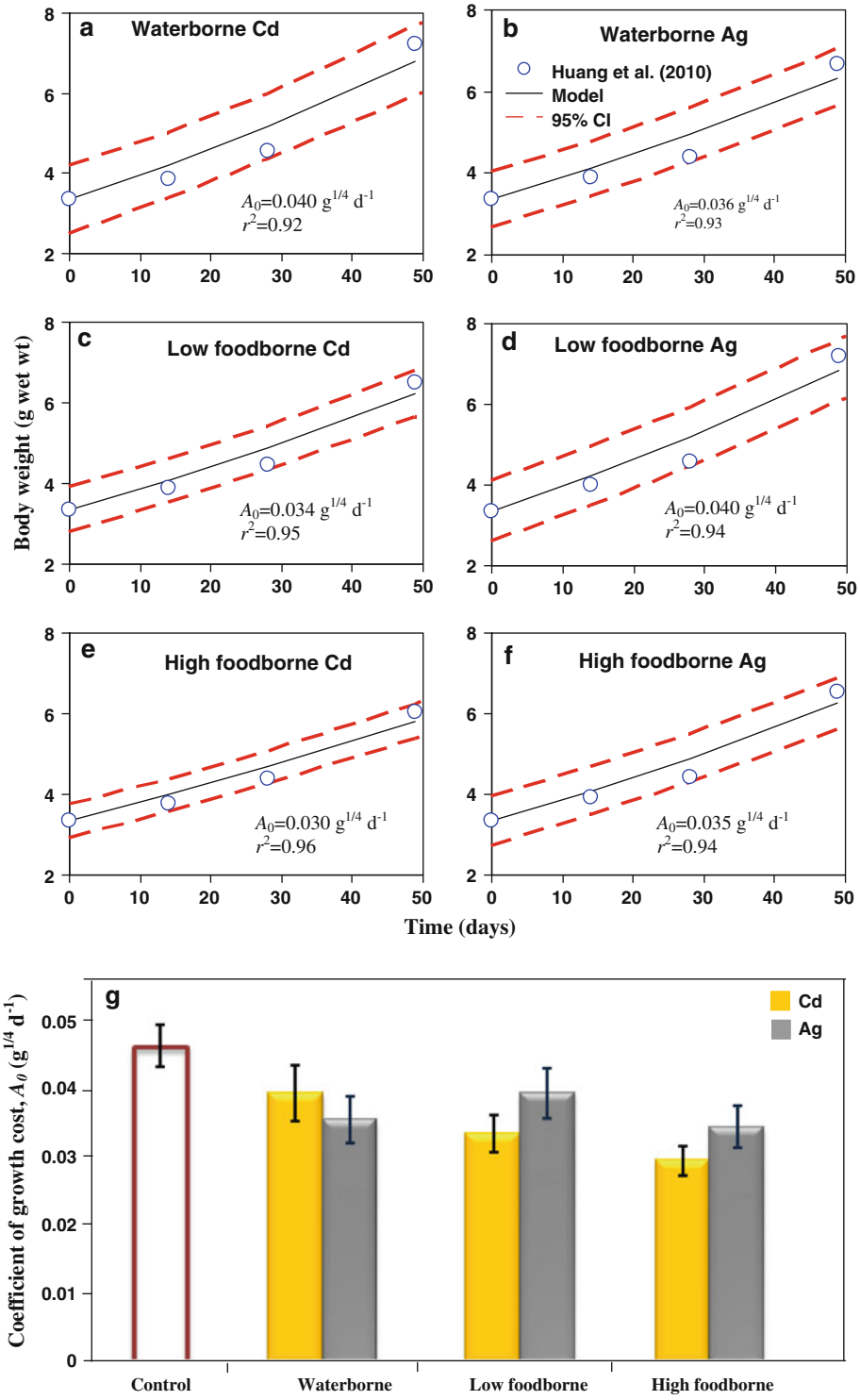

Fig. 7 Optimal fittings of the growth toxicity model [Eq. (5)] to the empirical physiological model [Eqs. (9) and (10)] based estimated growth biomass data in different **a** waterborne Cd and **b** Ag, **c** low foodborne Cd and **d** Ag, and **e** high foodborne Cd and **f** Ag exposure scenarios. **g** Growth cost coefficient of abalone subject to different Cd/Ag exposure scenarios

nearly threefold of magnitude higher than that of waterborne Ag. Furthermore, the k_r of foodborne Cd was also 2- to 8-folds of magnitude higher than that of foodborne Ag. Even the capacity to eliminate Cd was higher than that to eliminate Ag when the metal concentration was at a low level. However, our results indicated that abalone was able to resist Cd toxicity better than Ag toxicity.

When exposed to waterborne metal concentration at 50 μg L^{-1} Cd and 5 μg L^{-1} Ag, the accumulative burden of algae were 9.56 μg g^{-1} of Cd and 5.52 μg g^{-1} of Ag, respectively. Exposure of abalone to waterborne (50 μg l^{-1} Cd and 5 μg l^{-1} Ag) and low foodborne treatments (9.56 μg g^{-1} of Cd and 5.52 μg g^{-1} of Ag) resulted in similar exposure patterns as the above situations. Our

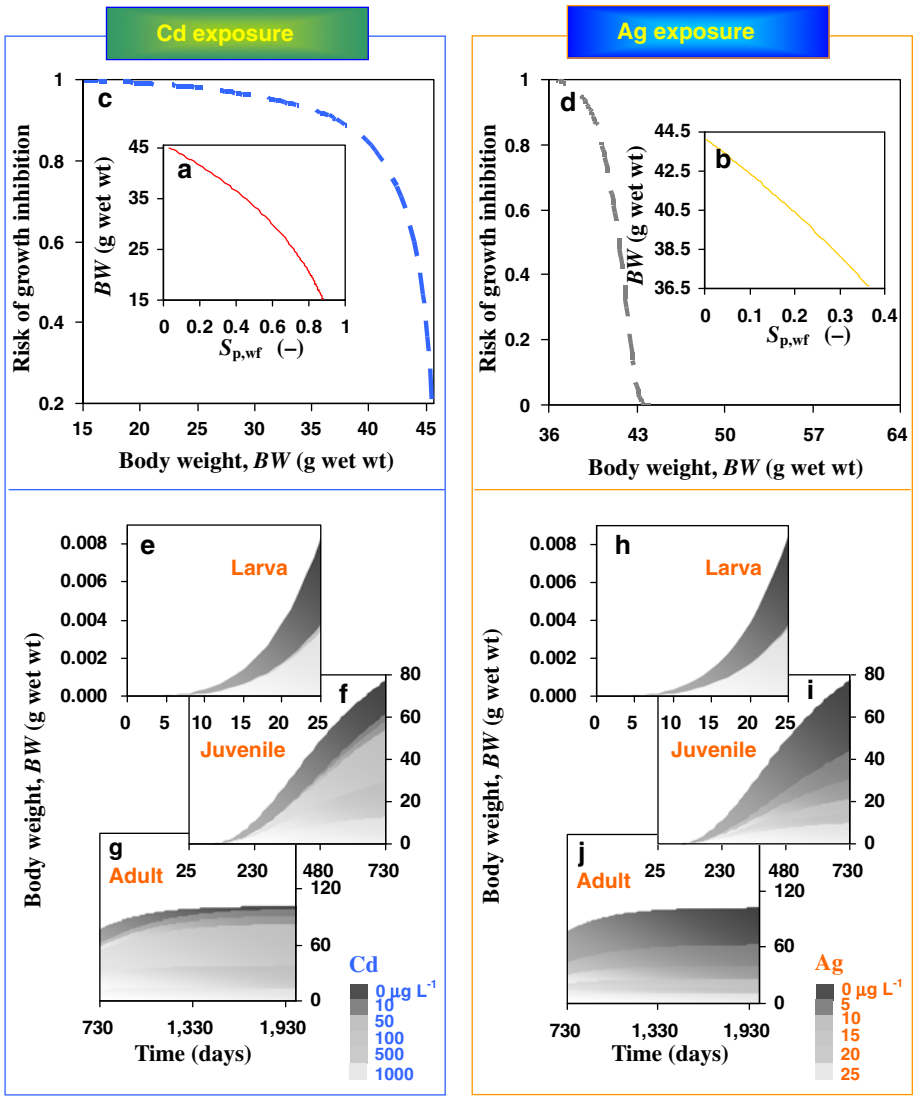

Fig. 8 Ecotoxicological risk assessment of abalone in Taiwan. **a** Relationships between biomass and susceptibility of abalone in water/foodborne Cd and **b** Ag exposure scenarios. **c** The risk probability of growth inhibition in water/foodborne Cd and **d** Ag exposure scenarios. **e–g** Simulation of biomass of abalone in each life-stage in water/foodborne Cd and **h–j** Ag exposure scenarios

results indicated that the coefficient of growth cost (A_0) of waterborne Cd (0.04 $g^{1/4}$ d^{-1}) was greater than that of low foodborne Cd (0.034 $g^{1/4}$ d^{-1}) at same concentration levels, whereas A_0 of waterborne Ag (0.036 $g^{1/4}$ d^{-1}) was lower than that of low foodborne Ag (0.04 $g^{1/4}$ d^{-1}). Huang et al. (2010) reported that when abalone were exposed to waterborne/foodborne Cd and Ag, the growth rate of shells and tissue significantly decreased, except in the low foodborne Ag treatment. Thus, the waterborne Cd toxicity effect was lower than that of the foodborne, whereas the waterborne Ag toxicity effect was greater than that of the foodborne.

Long-term risk assessment improvement

This study adopted the 49 day-growth bioassay data of juvenile abalone to determine the probability distribution of growth inhibition risk for the whole life-span of abalone in Taiwan due to Cd and Ag stressors. The merit of the West growth model can elucidate the growth inhibition over the entire life cycle based upon the limited growth information at the juvenile stage for abalone exposed to Cd and Ag concentrations. We reconstructed the dose–response models for waterborne and foodborne Cd and Ag exposures and growth biomass variability. We concluded that for 10 µg l^{-1} Cd exposure, the maximum biomass was 0.0039, 61.61, and 98.88 g for larva, juvenile, and adult abalone, respectively, whereas the maximum biomass was 0.0038, 43.87, and 62.97 g for larvae, juveniles, and adults, respectively, exposed to Ag. By contrast, the abalone experienced more growth susceptibility to Ag than to Cd in each life-stage. Previous studies also indicated that a serious consequence for population living was the influence of chemicals on juveniles (Kammenga et al. 1996; Ramskov and Forbes 2008).

Previous studies have quantified the assimilation efficiencies of metals in predators fed on different preys

(Cheung and Wang 2005; Rainbow et al. 2007; Huang et al. 2008; Dubois and Hare 2009; Lapointe et al. 2009). This factor may control the metal trophic transfer level. The subcellular partitioning of metal in aquatic organisms will also influence trophically available metal (Wallace and Lopez 1996; Wallace and Luoma 2003; Cheung and Wang 2005). The main subcellular partitioning fractions of trophically available metal were organelles, heat-denatured proteins, and metallothionein-like proteins, which could be also used to predict the trophic transfer fraction (Wallace and Luoma 2003). Cheung and Wang (2005) indicated that Ag was mostly concentrated in the insoluble fraction, whereas Cd had highest percentage of accumulation in soluble fraction of prey. If this critical metal subcellular partitioning information was available, the subcellular partitioning that caused biomagnification in food chains could be better identified.

In conclusion, this study incorporated the bioconcentration of metal in water with the biomagnification of metal in food to assess accurately long-term growth inhibition risk of abalone in an integrated scheme of toxicokinetics/toxicodynamics and subcellular partitioning. We anticipated that a combination of DAM, West growth model, and SPM can shape the framework to predict the potential growth biomass variability of abalone subjected to Cd and Ag stresses. This research may also provide mechanistic implications for optimizing a long-term ecotoxicological risk assessment in realistic situations.

References

Alunno-Bruscia M, van der Veer HW, Kooijman SALM (2009) The AquaDEB project (phase I): analysing the physiological flexibility of aquatic species and connecting physiological diversity to ecological and evolutionary processes by using dynamic energy budgets. J Sea Res 62:43–48

Ashauer R, Bozall ABA, Brown CD (2007) New ecotoxicological model to simulate survival of aquatic invertebrates after exposure of fluctuating and sequential pulses of pesticides. Environ Sci Technol 41:1480–1486

Borgmann U, Norwood WP, Dixon DG (2004) Re-evaluation of metal bioaccumulation and chronic toxicity in *Hyalella azteca* using saturation curves and the biotic ligand model. Environ Pollut 131:469–484

Buchwalter DB, Cain DJ, Martin CA, Xie L, Lunma SN, Garland T (2008) Aquatic insect ecophysiological traits reveal phylogenetically based differences in dissolved cadmium susceptibility. Proc Natl Acad Sci USA 105:8321–8326

Bury NR, Wood CM (1999) Mechanism of branchial apical silver uptake by rainbow trout is via the proton-coupled Na^+ channel. Am J Physiol 277:R1385–R1391

Castilho PC, Martins IA, Bianchini A (2001) Gill Na^+, K^+-ATPase and osmoregulation in the estuarine crab, *Chasmagnathus granulata* Dana, 1851 (Decapoda Grapsidae). J Exp Mar Bio Ecol 256:215–227

Chen HC (1989) Farming the small abalone *Haliotis diversicolor supertexta* in Taiwan. In: Hahn HO (ed) Handbook of culture of abalone and other marine gastropods. CRC Press, Boca Raton, pp 265–283

Cheung MS, Wang WX (2005) Influence of subcellular metal compartmentalization in different prey on the transfer of metal to a predatory gastropod. Mar Ecol Prog Ser 286:155–166

Croteau MN, Luoma SN (2009) Predicting dietborne metal toxicity from metal influxes. Environ Sci Technol 43:4915–4921

Di Toro DM, Allen HE, Bergman HL, Meyer JS, Paquin PR, Santore RC (2001) A biotic ligand model of the acute toxicity of metal I. Technical basis. Environ Toxicol Chem 20:2383–2396

Dubois M, Hare L (2009) Subcellular distribution of cadmium in two aquatic invertebrates: change over time and relationship to Cd assimilation and loss by a predatory insect. Environ Sci Technol 43:356–361

Gordon HR, Cool PA (2001) World abalone supply, markets and pricing: historical, current and future. J Shellfish Res 20: 567–570

Grosell M, Blanchard J, Brix KV, Gerdes R (2007) Physiology is pivotal for interactions between salinity and acute copper toxicity to fish and invertebrates. Aquat Toxicol 84:162–172

Hsieh HC (2005) Studies on the nutrition and heavy metals absorption of *Gracilaria coronopifolia* and *Gelidium amansii* at different salinity. Unpublished MS dissertation. National Taiwan Ocean University

Huang KM (1998) The culture of abalone. Council of Agriculture Executive Yuan, Taipei

Huang X, Ke C, Wang WX (2008) Bioaccumulation of silver, cadmium and mercury in the abalone *Haliotis diversicolor* from water and food sources. Aquaculture 283:194–202

Huang X, Guo F, Ke C, Wang WX (2010) Responses of abalone *Haliotis diversicolor* to sublethal exposure of waterborne and dietary silver and cadmium. Ecotoxicol Environ Saf 73:1130–1137

Janes N, Playle RC (1995) Modeling silver binding to gills of rainbow trout (*Oncorhynchus mykiss*). Environ Toxicol Chem 14:1847–1858

Jarayabhand P, Pahavasit N (1996) A review of the culture of tropical abalone with species reference to Thailand. Aquaculture 140: 159–168

Cheng JH (2004) The study of trace metals of the aquaculture ponds in Taiwan Area. Unpublished MS dissertation. National Taiwan Ocean University

Kammenga JE, Busschers M, Van Straalen NM, Jepson PC, Bakker J (1996) Stress induced fitness reduction is not determined by the most sensitive life-cycle trait. Funct Ecol 10:106–111

Kooijman SALM, Bedaux JJM (1996) The analysis of aquatic toxicity data. VU University press, Amsterdam

Lapointe D, Gentes S, Ponton DE (2009) Influence of prey type on nickel and thallium assimilation, subcellular distribution and effects in juvenile fathead Minnows (*Pimephales promelas*). Environ Sci Technol 43:8665–8670

Lee JH, Landrum PE, Koh CH (2002) Prediction of time-dependent PAH toxicity in *Hyalella azteca* using a damage assessment model. Environ Sci Technol 36:3131–3138

Mclusky DS, Bryant V, Cambell R (1986) The effects of temperature and salinity on the toxicity of heavy metals to marine and estuarine invertebrates. Oceanogr Mar Biol 24:481–520

Morgan IJ, Henry RP, Wood CM (1997) The mechanism of acute silver nitrate toxicity in freshwater rainbow trout (*Oncorhynchus mykiss*) is inhibition of gill Na^+ and Cl^- transport. Aquat Toxicol 38:145–163

Nadella SR, Fitzpatrick JL, Franklin N, Bucking C, Smith S, Wood CM (2009) Toxicity of dissolved Cu, Zn, Ni and Cd to developing embryos of the blue mussel (*Mytilus trossolus*) and the protective effect of dissolved organic carbon. Comp Biochem Physiol C –Toxicol Pharmacol 149:340–348

Ng TYT, Wood CM (2008) Trophic transfer and dietary toxicity of Cd from the oligochaete to the rainbow trout. Aquat Toxicol 87:47–59

Ng TYT, Klinck JS, Wood CM (2009) Does dietary Ca protect against toxicity of a low dietborne Cd exposure to rainbow trout? Aquat Toxicol 91:75–86

Nichols JW, Brown S, Wood CM, Walsh P, Playle RC (2006) Influence of salinity and organic matter on silver accumulation in Gulf toadfish (*Opsanus beta*). Aquat Toxicol 78:253–261

Oakes FR, Ponte RD (1996) The abalone market: opportunities for cultured abalone. Aquaculture 140:187–195

Pan K, Wang WX (2008) The subcellular fate of cadmium and zinc in the scallop *Chlamys nobilis* during waterborne and dietary metal exposure. Aquat Toxicol 90:253–260

Playle RC, Dixon DG, Burnison K (1993) Copper and cadmium binding to fish gill: estimates of metal-gill stability constants and modeling of metal accumulation. Can J Fish Aquat Sci 50: 2678–2687

Rainbow PS (2002) Trace metal concentration in aquatic invertebrates: why and so what? Environ Pollut 120:497–507

Rainbow PS, Amiard JC, Amiard-Triquet C, Cheung MS, Zhang L, Zhoung H, Wang WX (2007) Trophic transfer of trace metal: subcellular compartmentalization in bivalve prey, assimilation by gastropod predator and in vitro digestion simulations. Mar Ecol Prog Ser 348:125–138

Ramskov T, Forbes VE (2008) Life history and population dynamics of the opportunistic polychaete *Capitella* sp. I in relation to sediment organic matter. Mar Ecol Prog Ser 369:181–192

Seebaugh DR, Wallace WG (2009) Assimilation and subcellular partitioning of elements by grass shrimp collected along an impact gradient. Aquat Toxicol 93:107–115

Slaveykova VI, Wilkinson KJ (2005) Predicting the bioavailability of metals and metal complexes: Critical review of the biotic ligand model. Environ Chem 2:9–24

Stumm W, Morgan JJ (1996) Aquatic Chemistry, 3rd edn. Wiley-Interscience, New York

Tsai JW, Liao CM (2006) Mode of action and growth toxicity of arsenic to tilapia *Oreochromis mossambicus* can be determined bioenergetically. Arch Environ Contam Toxicol 50:144–152

Voets J, Redeker ES, Blust R, Bervoets L (2009) Differences in metal sequestration between zebra mussels from clean and polluted field locations. Aquat Toxicol 93:53–60

Wallace WG, Lopez GR (1996) Relationship between subcellular cadmium distribution in prey and cadmium trophic transfer to a predator. Estuaries Coasts 19:923–930

Wallace WG, Luoma SN (2003) Subcellular compartmentalization of Cd and Zn in two bivalves. II. Significance of trophically available metal (TAM). Mar Ecol Prog Ser 257:125–137

Wang WX, Rainbow PS (2006) Subcellular partitioning and the prediction of cadmium to toxicity to aquatic organisms. Environ Chem 3:395–399

Ward TJ, Kramer JR (2002) Silver speciation during chronic toxicity tests with the mysid, *Americanmysis bahia*. Comp Biochem Physiol C Toxicol Pharmacol 133:75–86

West GB, Brown JH, Enquist BJ (2001) A general model for ontogenetic growth. Nature 413:628–631

Wood CM, McDonald MD, Walker P, Grosell M, Barimo JF, Playle RC, Walsh PJ (2004) Bioavailability of silver and its relationship to ionoregulation and silver speciation across a range of salinities in the gulf toadfish (*Opsanus beta*). Aquat Toxicol 70:137–157